Magnetic imaging of the paramagnetic Meissner effect in the granular high-T_c superconductor $Bi_2Sr_2CaCu_2O_x$

1998 J. Phys.: Condens. Matter 10 L97

(http://iopscience.iop.org/0953-8984/10/6/001)

J. Phys.: Condens. Matter **10** (1998) L97–L103. Printed in the UK PII: S0953-8984(98)90009-1

LETTER TO THE EDITOR

Magnetic imaging of the paramagnetic Meissner effect in the granular high-T_c superconductor $Bi_2Sr_2CaCu_2O_x$

J R Kirtley†, A C Mota‡, M Sigrist§ and T M Rice‖

† IBM Research, Yorktown Heights, NY 10598, USA
‡ Festkörperphysik, ETH-Hönggerberg, 8093 Zürich, Switzerland
§ Yukawa Institute for Theoretical Physics, Kyoto University, Kyoto 606-01, Japan
‖ Theoretische Physik, ETH-Hönggerberg, 8093 Zürich, Switzerland

Received 1 December 1997

Abstract. We have imaged the spatial distribution of magnetic flux on a granular sample of the high-temperature superconductor $Bi_2Sr_2CaCu_2O_x$ using a scanning SQUID microscope. Our results establish the presence of spontaneous orbital magnetic moments which were suggested to be the origin of the paramagnetic response of these materials. The signature of the orbital magnetic moments is a rather broad distribution of local magnetic fields at the surface of the sample. A simple model for the distribution is presented.

Conventional superconductors generally tend to expel a small external magnetic field upon cooling into the superconducting state. This Meissner effect leads to complete, or (due to remnant trapped flux, e.g. in a ceramic sample composed of grains and voids) partial, diamagnetism. Therefore it came as a surprise when a paramagnetic signal was observed in ceramic $Bi_2Sr_2CaCu_2O_x$ (Bi-2212) [1–4]. The origin of the paramagnetism has been a controversial subject. Braunisch *et al* [4] and Kusmartsev [5] proposed that some form of spontaneous orbital currents were responsible, giving rise to magnetic moments which could be aligned by the external field. This proposal for spontaneous orbital currents (Wohlleben effect) in turn led two of us [6, 7] to propose that an intrinsic $d_{x^2-y^2}$-wave symmetry of the superconducting state would naturally lead to frustrated Josephson junction circuits in a ceramic sample where randomly oriented grains contact each other [8]. Although spontaneous orbital currents have now been unequivocally demonstrated for high-temperature superconductors in controlled geometries, and the evidence for $d_{x^2-y^2}$-wave symmetry is now overwhelming [9–15], the controversy has continued. In part this is due to the observation of paramagnetic signals under quite different conditions, e.g. in bulk Nb samples [16–19]. In this letter we report the first direct imaging of the local magnetic flux distribution in the ceramics by a scanning SQUID microscope (SSM) and demonstrate that a polarization of the distribution of spontaneous fluxes is indeed responsible for the paramagnetic signal.

Before proceeding to a discussion of our experiment we would like to remark that these two forms of paramagnetism in ceramic Bi2212 and in a bulk Nb sample can be clearly distinguished in several other ways. For example, the cooling rate affects the magnetic response differently in the two cases. Recent experimental data show significant differences between Nb and granular $Bi_2Sr_2CaCu_2O_x$ (Bi2212) samples. While slow cooling enhances the paramagnetic signal for the granular sample, it is diminished in the Nb sample. This clearly indicates that the equilibrium state of both samples in a small magnetic field is

0953-8984/98/060097+07$19.50

quite different [20]. For the Nb discs Koshelev and Larkin gave an explanation based on the idea that during the cooling process the surface region nucleates superconductivity before the bulk, so that magnetic flux in the sample is compressed and creates an enhanced magnetization [21]. This compressed flux mechanism leads to a metastable state which depends on the cooling procedure whereas the polarization of the spontaneous orbital moments is an equilibrium process. Further, noise measurements of the magnetization of Bi2212 give signals which are compatible with the presence of spontaneous orbital moments [22].

We used a sample whose preparation, characterization and measurement of the magnetization were reported previously [4]. The magnetic images were made with a high-resolution SSM [23]. This instrument uses an Nb–Al_2O_3–Nb low-T_c SQUID fabricated on a silicon substrate. The substrate is polished to a sharp tip spaced a few tens of micrometres from a well shielded superconducting pickup loop, which is an integral part of the SQUID. The SQUID substrate is mounted on a flexible cantilever, oriented at a shallow angle, typically 20 degrees relative to the sample surface, and the sample is scanned relative to the SQUID, with the tip of the substrate in direct contact with the sample. For these measurements the sample was polished to a mirror finish, and both sample and SQUID were coated with a thin layer to protect the SQUID substrate from abrasion. We estimate, from fits of Abrikosov vortices imaged using similar tip geometry and SQUID and sample coating techniques, that the spacing between the pickup loop and the surface of the superconducting sample is about 5 μm. The SQUID signal is proportional to the magnetic flux through the loop area. The present images were taken with a square pickup loop. In this geometry a single bulk Abrikosov vortex couples about $0.5\Phi_0$ ($\Phi_0 = h/2e$) through the 8.2 μm$\times$8.2 μm area of the pickup loop located directly above it.

Figure 1(a)–(f) shows a series of SSM images of the Bi2212 sample which was cooled through the superconducting transition temperature ($\approx$84 K) at different values of an externally applied magnetic field. The images were taken with the field still applied and the sample and SQUID immersed in liquid helium at 4.2 K. Each image is of a square area 3 mm on a side. The outlined square shows the 480 μm $\times$ 480 μm area of the images used to generate the histograms of figure 2. We analyse only this area, because our SQUID has two magnetic field sensitive regions: the pickup loop, and the hole in the superconducting ground plane for the flux modulation coil [23, 24]. The images were taken with the SQUID oriented vertically, with the pickup loop towards the top of the images. Therefore, when the pickup loop covers the region outlined, the modulation hole senses areas well off the sample (below the bottom of the image), and simply contributes a constant background signal to the image.

In figure 1 we show the spatial distribution of the magnetic flux in and around the sample. The grey contrast scale is chosen so that white corresponds to the largest and black to the smallest (often negative) flux value. In all cases the flux is plotted relative to the flux introduced by the external field, which sets the grey level away from the sample. One overall feature observable by eye is the difference between the paramagnetic magnetization (sample is brighter than the background) at weak fields, and a diamagnetic signal (sample is darker than the background), in the pickup loop at strong fields. For weak external fields the inhomogeneity of the magnetic flux is clearly visible and gives rise to a broad distribution of the local fluxes.

The flux distributions relative to the external flux measured in the outlined square are shown as histograms in figure 2. The distribution is broad, as anticipated above, and the average value indicates the overall response, which is paramagnetic for weak fields. In table 1 we list the average flux $\Phi_{av} - \Phi_{ext}$ and the standard deviation $\delta\Phi = \langle(\Phi - \Phi_{av})^2\rangle^{1/2}$

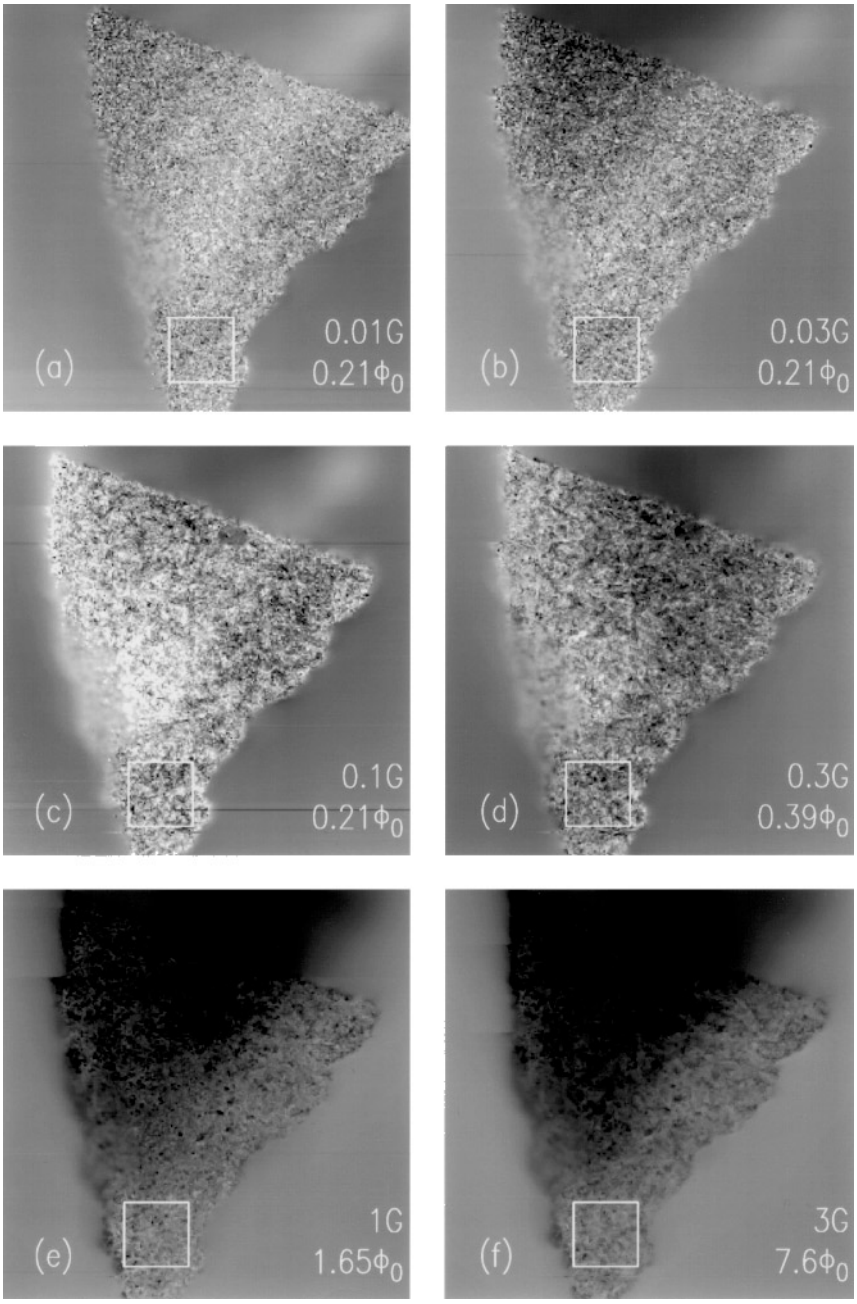

Figure 1. Scanning SQUID microscope images of a granular Bi2212 sample, cooled and imaged in various fields. Each image has 512×512 pixels, with 6 μm per pixel. The individual images are labelled by the cooling field, and by the maximal range of variation of the flux (in units of Φ_0) in each case. The outlined areas are regions of the images analysed further in the histograms of figure 2.

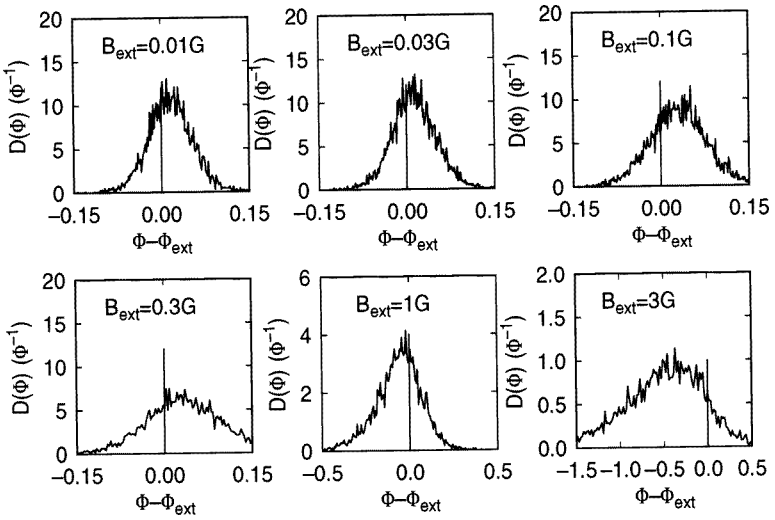

Figure 2. Histograms of the distribution of occurrence of each SQUID flux value in the outlined areas of figure 1, normalized so that the integral yields unity. Each panel is labelled by the cooling field in Gauss. The horizontal axes correspond to the flux through the SQUID at a particular spot on the sample, relative to the background with the pickup loop far from the sample, i.e. $\Phi - \Phi_{ext}$.

Table 1. Average flux $\Phi_{av} = \langle \Phi - \Phi_{ext} \rangle$ measured in the SSM and standard deviation $\delta\Phi = \langle (\Phi - \Phi_{av})^2 \rangle^{1/2}$ for different applied fields.

H_{ext}	Φ_{av}/Φ_0	$\delta\Phi/\Phi_0$
10 mOe	0.0157	0.0384
30 mOe	0.0128	0.0386
100 mOe	0.0299	0.0494
300 mOe	0.0318	0.0675
1 Oe	−0.0676	0.139
3 Oe	−0.51	0.465

(Φ_{ext} denotes the flux of the external field through the pickup loop).

We first compare our SSM data with the total magnetization measurement of the whole sample [4]. Both show the same qualitative dependence on the low-temperature magnetization on the applied field (see figure 3). In particular, the sign of the magnetization changes for both measurements at the same field value $B_{ext} \approx 0.6$ G. This confirms that the SSM data, scanning only a part of the sample, are typical of the magnetization of the whole sample. Let us now turn to the width of the flux distribution, i.e. the standard deviation from the average flux. The field dependence of $\delta\Phi$ indicates the existence of spontaneous flux at low external fields. If the flux observed were entirely due to flux trapped and compressed between and inside the grains, then we expect that both Φ_{av} and $\delta\Phi$ would tend to zero in the zero-field limit. This is, however, not the case as we illustrate in figure 3, where we observe that the zero-field limit of $\delta\Phi$ is finite. This can be readily interpreted if we assume that the flux distribution at low fields is mostly due to spontaneous orbital currents for low external fields, which can flow in either direction. Thus we expect to see an inhomogeneous field pattern even at zero external field. The broadening of the flux distribution with increasing

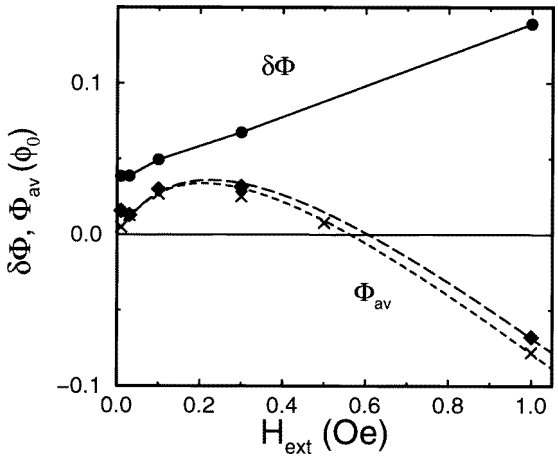

Figure 3. Standard deviation of the flux distribution $\delta\Phi = \langle(\Phi - \Phi_{av})^2\rangle^{1/2}$ (circles, solid line) as a function of the external field. The average flux Φ_{av} of the SSM measurement (diamonds, long-dashed line) compares well with the appropriately scaled magnetization of the whole sample (x, dashed line) [4].

field can be understood as due to flux trapping and Meissner effect of the grains. Generally more magnetic flux concentrates in the voids and essentially little flux is trapped inside the grains. This leads to an enhancement of the contrast in the flux values for large external fields and, consequently, to a broader distribution.

For the low-field regime the flux distribution can be easily simulated using a model for the boundary between many grains. Such a grain boundary can be considered as a long Josephson junction and may be described by a sine–Gordon equation [25],

$$\frac{\partial^2\varphi}{\partial x^2} = \frac{1}{\lambda_J^2}\sin(\varphi(x) + \theta(x)) \tag{1}$$

where φ is the Josephson phase difference on the grain boundary and λ_J is the Josephson penetration depth. The presence of 0- and π-junctions enters through $\theta(x)$, which assumes the values 0 or π as a function of the position x along the grain boundary. This model is simulated on a system of length L using N mesh points to determine $\varphi(n)$ for fixed values of $\theta(n)$ [26]. The local flux $\Phi(n)$ between mesh point n and $n-1$ is given by $\Phi(n) = \Phi_0(\varphi(n) - \varphi(n-1))/2\pi$. The external field is introduced via the boundary conditions at the two ends of the junction $(\varphi(N) - \varphi(N-1))/2\pi = (\varphi(2) - \varphi(1))/2\pi = B_{ext}L/N\Phi_0$. Using a relaxation method [26], we calculate φ while gradually lowering the temperature by introducing decreasing values of λ_J. In figure 4 we show the flux distribution obtained for the case of $L = 100$, $N = 1000$, starting with $\lambda_J = 40$, which is decreased by successive division by 2 to a final value of 0.156. The low external field is $B_{ext} = 0.1\Phi_0/Ld$ (d is the magnetic width of the junction). We obtain a broad distribution with a shape that is qualitatively similar to the experiment. The phase φ has essentially a random-walk-like dependence on x so that the histogram has an approximately Gaussian distribution. Within this simple model we can describe the generation of spontaneous flux and the interaction effects between flux lines. However, the broadening of the flux distribution with increasing field is not properly reproduced because the contrast between trapped flux and the screening grains is not taken into account.

In summary we would like to emphasize that the low-field data obtained by an SSM

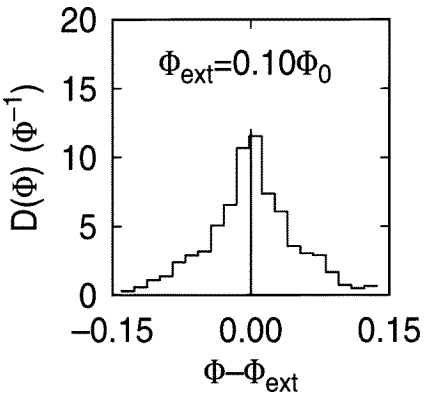

Figure 4. Histogram for the small-field limit of the sine–Gordon model described in the text.

on a granular Bi2212 sample are in very good qualitative agreement with the previous magnetization measurements and, in addition, provide direct evidence for the presence of spontaneous orbital current. On the other hand, independent evidence [20, 22] indicates that the paramagnetic signal in Nb samples has a different mechanism, probably the one proposed by Koshelev and Larkin [21]. It is not possible from this SSM measurement alone to determine the origin of the orbital currents. However, a series of previous experiments suggest strongly that grain boundaries with intrinsic π-phase shifts are appearing in these high-temperature superconductors and are very likely responsible for the paramagnetic response [9–15]. In this sense, the paramagnetic response (Wohlleben effect) in granular Bi2212 systems is consistent in all aspects with an explanation based on $d_{x^2-y^2}$-wave pairing symmetry [6, 7, 27].

We are very grateful to the late D Wohlleben for attracting our attention to this effect and for providing us with a sample produced by members of his group. We would also like to thank M B Ketchen, M Bhushan and A W Ellis for assistance in the design and fabrication of the microscope used in this work, and K A Moler and D J Scalapino for assistance in the development of the computer program used for the simulation presented here. This work was supported by the Swiss Nationalfonds.

References

[1] Svendlindh P *et al* 1989 *Physica* C **162–164** 1365
[2] Lee W W, Huang Y T, Lu S W, Chen K and Wu P T 1990 *Solid State Commun.* **74** 97
[3] Lan M D, Liu J Z and Shelton R N 1991 *Phys. Rev.* B **43** 12 989
[4] Braunisch W *et al* 1993 *Phys. Rev.* B **48** 4030
[5] Kusmartsev F V 1992 *Phys. Rev. Lett.* **69** 2268
[6] Sigrist M and Rice T M 1992 *J. Phys. Soc. Japan* **62** 4283
[7] Sigrist M and Rice T M 1995 *Rev. Mod. Phys.* **67** 503
[8] Geshkenbein V B, Larkin A I and Barone A 1987 *Phys. Rev.* B **36** 235
[9] Wollman D A *et al* 1993 *Phys. Rev. Lett.* **71** 2134
[10] Brawner D A and Ott H R 1994 *Phys. Rev.* B **50** 6530
[11] Tsuei C C *et al* 1994 *Phys. Rev. Lett.* **73** 593
[12] Wollman D A 1995 *Phys. Rev. Lett.* **74** 797
[13] Miller J H Jr *et al* 1995 *Phys. Rev. Lett.* **74** 2347
[14] Mathai A *et al* 1995 *Phys. Rev. Lett.* **74** 4523
[15] Kousnetsov K A *et al* 1997 *Phys. Rev. Lett.* **79** 3050

[16] Minhaj M S M *et al* 1995 *Phys. Rev. Lett.* **75** 529
[17] Kostić P *et al* 1996 *Phys. Rev.* B **53** 791
[18] Rice T M and Sigrist M 1997 *Phys. Rev.* B **55** 14 647
[19] Kostić P *et al* 1997 *Phys. Rev.* B **55** 14 649
[20] Gross R 1997 private communication
[21] Koshelev A E and Larkin A I 1995 *Phys. Rev.* B **52** 13 559
[22] Magnusson J, Nordblad P and Svedlindh P 1997 *Physica* C **282–287** 2369
[23] Kirtley J R *et al* 1995 *Appl. Phys. Lett.* **66** 1138
[24] Usually this extra pickup area is not apparent, since it is 1.2 mm away from the loop, well removed from the sample, where the magnetic fields are slowly varying. However, in this experiment, the scanned areas are relatively large (length 3 mm), so that the background effect is visible in the images. The influence of this additional pickup is clearly seen, for example, as the dark shadow at the top of figure 1(f).
[25] Owen C S and Scalapino D J 1967 *Phys. Rev.* **164** 538
[26] Kirtley J R, Moler K A and Scalapino D J 1997 *Phys. Rev.* B **56** 886
[27] Recently an interesting surface contribution to the paramagnetic susceptibility of d-wave superconductors was discussed by Higashitani S 1997 *J. Phys. Soc. Japan* **66** 2556